Supporting Information

High-crystallinity fluoropolymer collaborating fluorous solvent post-treatment for efficient thick-film organic solar cells

*Zhilong He,[1] Siyuan Li,[1] Zhe Hao,[1] Yi Lin,[2] Zheng Tang,[2] and Hongliang Zhong [1,2,]**

[1] School of Chemistry and Chemical Engineering, Shanghai Jiao Tong University, Shanghai 200240, China.

[2] State Key Laboratory of Advanced Fibers Materials, Center for Advanced Low-dimension Materials, College of Materials Science and Engineering, Donghua University, Shanghai 201620, China.

E-mail: hlzhong@dhu.edu.cn

Materials and Synthesis

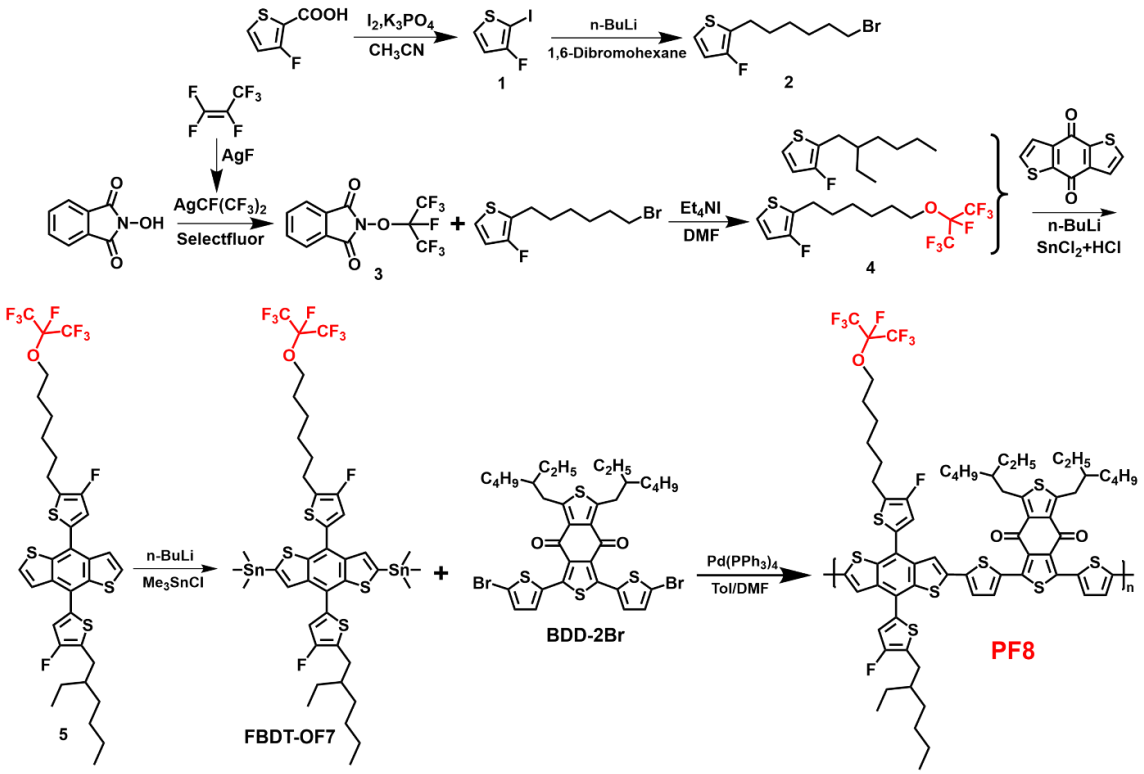

Scheme S1. Synthesis route of polymer PF8.

All commercially available chemicals and solvents was purchased from Aladdin, Bidepharm, and Sigma-Aldrich Co., Ltd and used without further purification. Hexafluoropropylene, selectfluor and perfluorotoluene are obtained from Shangfluoro Technology Co., Ltd. 3-fluoro-2-(2-ethylhexyl)-thiophene and BDD-2Br are purchased from Derthon Optoelectronics Materials Science Technology Co., Ltd. BDT-F and Benzo[1,2-b;4,5-b']dithiophene-4,8-dione are acquired from Nanjing Zhiyan Technology Co.,Ltd. The detailed synthetic procedure are shown in **Scheme S1**.

3-fluoro-2-iodothiophene (Compound 1)

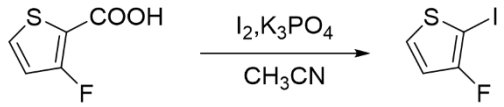

Under argon protection, 3-fluoro-2-thiophenecarboxylic acid (2.92 g, 20 mmol), potassium phosphate (8.50 g, 40 mmol), and iodine (20.32 g, 80 mmol) were dissolved in 100 mL anhydrous acetonitrile and refluxed at 100 ℃ for 24 h. The organic layer was extracted with petroleum ether and washed with sodium bisulfite aqueous solution three times. After removing solvent by rotary evaporation, the crude product was purified by silica gel column chromatography with petroleum ether afforded light-yellow oil (3.83 g, 83.9%). ^{1}H NMR (400 MHz, $CDCl_3$, 25 ℃), δ (ppm): 7.41 (dd, J = 5.9, 4.0 Hz, 1H), 6.70 (dd, J = 5.8, 4.0 Hz, 1H).

2-(6-bromohexyl)-3-fluorothiophene (Compound 2)

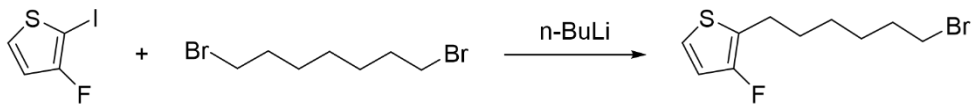

A solution of 3-fluoro-2-iodothiophene (3.42 g, 15 mmol) was dissolved in 50 mL anhydrous tetrahydrofuran and n-BuLi (2.4 M in hexane, 6.9 mL, 16.5 mmol) was added into the solution in dropwise at -78 ℃. After stirred at -78 ℃ for 1 h, 1,6 dibromohexane (4.39 g, 18 mmol) was added dropwise at -78 ℃, then recovered to room temperature and stirred overnight. After quenching the reaction, the organic layer was collected through extracting with petroleum ether and dried over

anhydrous $MgSO_4$. The residue was further purified by silica gel column chromatography with petroleum ether, giving a colorless oil (3.02 g, 75.9%). ^{1}H NMR (400 MHz, $CDCl_3$, 25 ℃), δ (ppm): 6.97 (dd, J = 5.6, 3.8 Hz, 1H), 6.73 (dd, J = 5.8, 2.0 Hz, 1H), 3.18 (t, J = 7.0 Hz, 2H), 2.76-2.68 (m, 2H), 1.83 (p, J = 7.0 Hz, 2H), 1.69-1.54 (m, 2H), 1.47-1.34 (m, 4H).

2-((Perfluoropropan-2-yl)oxy)isoindoline-1,3-dione (Compound 3)

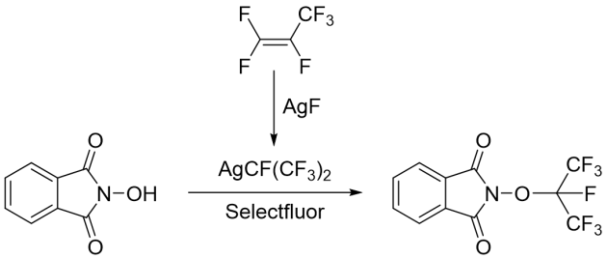

To a solution of silver fluoride (7.62 g, 60 mmol) in 100 mL dry anhydrous acetonitrile, hexafluoropropylene (balloon, 1 atm, 27.0 g, 180 mmol) was added and the mixture was stirred at ambient temperature in the dark until silver fluoride precipitate dissolved completely. Subsequently, this solution was added slowly to another oven-dried vessel, which was filled with selectfluor (21.24 g, 60 mmol) and *N*-hydroxyphthalimide (4.89 g, 30 mmol). The reaction mixture was stirred overnight at ambient temperature. After removing solvent by rotary evaporation, and the crude product was purified by silica gel column chromatography (petroleum ether: EtOAc = 10:1) to give a white solid (8.36 g, 84.2%). ^{1}H NMR (400 MHz, $CDCl_3$, 25 ℃), δ (ppm): 7.95 (dd, J = 5.5, 3.1 Hz, 2H), 7.86 (dd, J = 5.6, 3.1 Hz, 2H). ^{19}F NMR (376 MHz, $CDCl_3$, 25 ℃), δ (ppm): -78.26 (6F), -139.46 (1F).

Compound 4

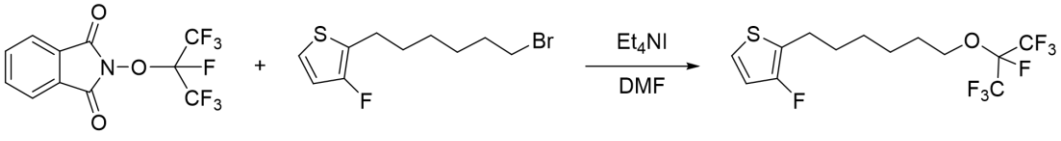

Under argon protection, compound 2 (1.32 g, 5 mmol), compound 3 (2.48 g, 7.5 mmol), and Et_4NI (0.93 g, 2.5 mmol) were dissolved in 50 mL anhydrous *N*,*N*-dimethylformamide (DMF) and stirred at 80 ℃ for 12 h. After cooling to room temperature, the reaction was washed with $Na_2S_2O_4$

aqueous solution and extracted with petroleum ether. The organic layer was washed with brine and dried over $MgSO_4$, then filtered and concentrated in vacuo to give a residue. The residue was purified by silica gel column chromatography with petroleum ether to afford compound 4 as a colorless oil (1.38 g, 74.5%). ^{1}H NMR (400 MHz, $CDCl_3$, 25 ℃), δ (ppm): 6.97 (dd, J = 5.6, 3.8 Hz, 1H), 6.73 (d, J = 5.5 Hz, 1H), 3.97 (t, J = 6.4 Hz, 2H), 2.72 (t, J = 7.5 Hz, 2H), 1.72-1.61 (m, 4H), 1.43-1.38 (m, 4H). ^{19}F NMR (376 MHz, $CDCl_3$, 25 ℃), δ (ppm): -79.00 (6F), -135.89 (1F), -142.10 (1F).

Compound 5

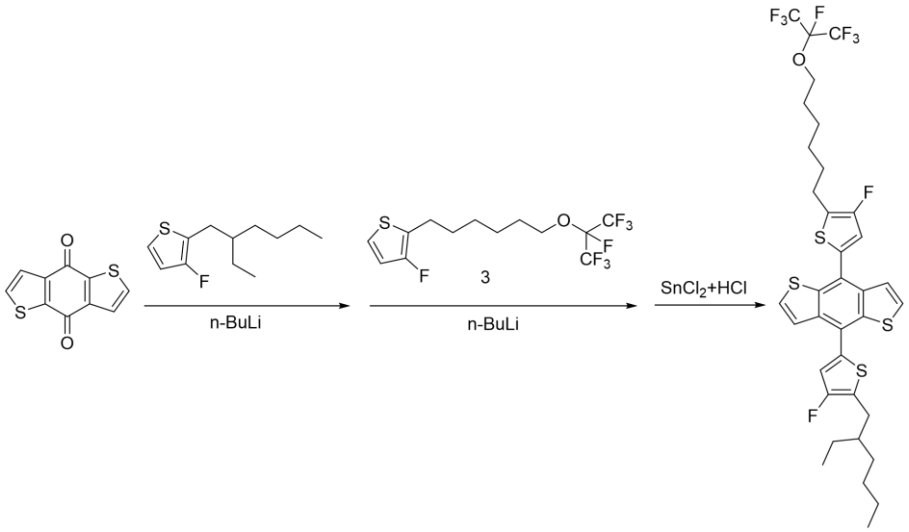

Compound 3 (1.11 g, 3 mmol) and 25 mL dry THF were added into a schlenk flask under Ar protection. The solution was cooled to -78 ℃ and n-BuLi (2.4 M, 1.45 mL, 3.45 mmol) was added dropwise and stirred at -78 ℃ for 30 min. Afterwards, 3-fluoro-2-(2-ethylhexyl)-thiophene (0.64 g, 3 mmol) and 25 mL dry THF were added into the mixture solution and then cooled to -78 ℃. Subsequently, n-BuLi (2.4 M, 1.45 mL, 3.45 mmol) was added dropwise and warmed to room temperature and stirred for 1 h. Benzo[1,2-b;4,5-b']dithiophene-4,8-dione (0.62 g, 2.8 mmol) was added to the solution and stirred at 50 ℃ for another 2 h. After cooling to ambient temperature, the mixture of $SnCl_2$ (2.28 g, 12 mmol) in 10% HCl (20 mL) was added, and the mixture was stirred at room temperature overnight. After that, the reaction mixture was poured into water and extracted with petroleum ether. The organic layer was washed with water for three times and dried over

$MgSO_4$. After the removal of solvent, the residue was purified by silica gel column chromatography (petroleum ether:DCM = 10:1) to afford pure product as a light yellow solid (0.93 g, 42.3%). ^{1}H NMR (400 MHz, $CDCl_3$, 25 ℃), δ (ppm): 7.64 (dd, J = 5.7, 2.9 Hz, 2H), 7.50 (d, J = 5.7 Hz, 2H), 7.14 (s, 1H), 4.01 (t, J = 6.4 Hz, 2H), 2.85 (t, J = 7.5 Hz, 2H), 2.79 (d, J = 6.8 Hz, 2H), 1.79-1.70 (m, 4H), 1.68-1.64 (m, 1H), 1.53-1.34 (m, 12H), 0.98-0.91 (m, 6H). ^{19}F NMR (376 MHz, $CDCl_3$, 25 ℃), δ (ppm): -78.96 (6F), -132.96 (1F), -133.33 (1F), -142.05 (1F).

FBDT-OF7

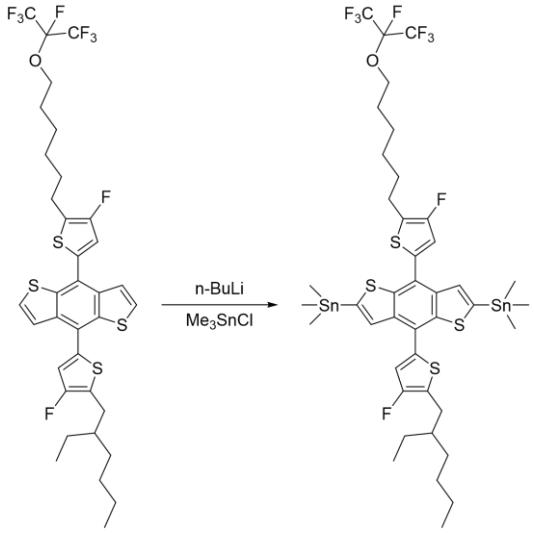

Compound 4 (0.77 g, 1 mmol) and 30 mL dry THF were mixed at -78 ℃ under argon protection, 1.1 mL n-BuLi (2.4 M in hexane, 2.6 mmol) was added dropwise and was then stirred at -78 ℃ for 1 h. Subsequently, 3.2 mL chlorotrimethtlstannane (1.0 M in hexane, 3.2 mmol) was added in several portions and the mixture was stirred for 6 h at ambient temperature. Then, the mixture was extracted with petroleum ether, the combined organic phase was washed with water three times and dried over Na_2SO_4. After the removal of solvent, the crude product was purified by recrystallization to obtain a light-yellow solid in low temperature and light-yellow oil in room temperature (0.89 g, 81.1%). ^{1}H NMR (400 MHz, $CDCl_3$, 25 ℃), δ (ppm): 7.67 (d, J = 3.8 Hz, 2H), 7.17 (s, 2H), 4.02 (t, J = 6.4 Hz, 2H), 2.87 (t, J = 7.6 Hz, 2H), 2.80 (d, J = 6.8 Hz, 2H), 1.78-1.74 (m, 4H), 1.72-1.68 (m, 1H), 1.52-1.36 (m, 12H), 0.98-0.90 (m, 6H), 0.43 (s, 18H). ^{19}F NMR (376 MHz, $CDCl_3$, 25 ℃), δ

(ppm): -78.96 (6F), -133.09 (1F), -133.43 (1F), -142.05 (1F). MS (MALDI-TOF) *m/z*: Calculated for [M^+] 1096.07; found: 1096.01.

Polymer PF8

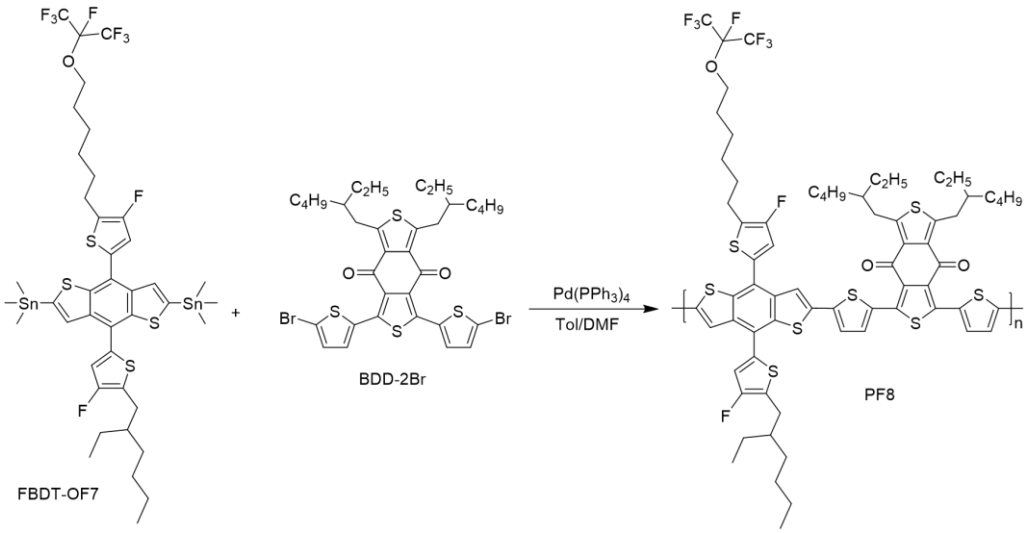

To a mixture of Compound 5 (109.7 mg, 0.1 mmol), BDD-2Br (76.7 mg, 0.1 mmol), $Pd(PPh_3)_4$ (4.62 mg, 0.004 mmol) in 4 mL dry toluene mixed solvent was degassed by three cycles of freeze-pump-thaw to remove O_2 and refluxed at 120 ℃ for 24 h. Then the solution was cooled to room temperature and added into 150 mL methanol dropwise. The precipitate was collected and further purified via Soxhlet extraction by using methanol, hexane, acetone, $CHCl_3$ and chlorobenzene in sequence. The chlorobenzene fraction was concentrated and added into methanol dropwise. The precipitate was collected and dried under vacuum overnight to give fluoropolymer PF8 (116 mg, 73.0%). GPC: M_n = 47.0 K, PDI = 2.24.

Characterization

^{1}H NMR and ^{19}F NMR spectra were collected on a Bruker AV-400 (400 MHz) spectrometers are given in ppm, the internal reference was the residual solvent resonance of $CDCl_3$. The molecular weight and polydispersity index were determined by Shimadzu-20A GPC. The polymer was dissolved in chlorobenzene at a concentration of 1.0 mg mL^{-1} and the mobile phase is hot chlorobenzene at 80 ℃ with a flow rate of 1.0 mL min^{-1}. The molecular weight is calculated based on standard polystyrene sample with narrow polydispersity. Theoretical calculations are performed

using Density Functional Theory (DFT) in the Gaussian16 code on the hybrid functional B3LYP/6-31G (d,p) basis set. UV-Vis absorption spectra of polymers or blends dissolved in $CHCl_3$ or spin-coated on quartz plates were recorded on the UV-2700 spectrophotometer. Cyclic voltammetry (CV) measurements of these products were conducted on a CHI660D electrochemical workstation in a standard three-electrode configuration, in which $Ag/AgNO_3$, Pt wire and modified GCE, were acted as reference, counter and working electrode, at a potential scanning rate of 50 mV/s in tetrabutylammonium hexafluorophosphate ($n\text{-}Bu_4NPF_6$, 0.1 M) acetonitrile solution. The ferrocene/ferrocene$^+$ (Fc/Fc^+) pair was utilized as the internal reference and its redox potential ($\varphi_{Fc/Fc+}$) was measured to 0.03 eV *vs.* $Ag/AgNO_3$. The HOMO and LUMO energy levels (E_{HOMO}/E_{LUMO}) of polymer can be estimated by the equations of $E_{HOMO}/E_{LUMO}=-e(E_{ox}/E_{red}+4.8-\varphi_{Fc/Fc+})$. Atomic force microscopy (AFM) images of specimens were detected by a Bruker Multimode 8 using tapping mode at room temperature. Grazing-incidence wide-angle X-ray scattering (GIWAXS) characterizations of films were carried out at the BL02U2 beamline of Shanghai Synchrotron Radiation Facility (SSRF). Samples were prepared under device fabrication conditions on the Si/PEDOT:PSS substrates. The X-ray beam (10 keV) was incident at a grazing angle of 0.15 °. The thicknesses of active layers were measured by a Filmetrics Profilm 3D Optical Step Profiler.

Device Measurements

The device *J-V* characteristics were tested by a Keithley 2420 SourceMeter unit in forward direction under AM 1.5 G irradiance (100 mW cm^{-2}) as generated by a 300 W Xe lamp solar simulator (Enlitech SS-F5-3A) at room temperature. The light intensity was calibrated using a standard Si diode with KG-5 filter. The EQE spectra was characterized using an Enlitech EQE system (Enlitech QE-M110) with a Si diode as the reference cell. Monochromatic light was generated from a 75 W Xe lamp with a monochromator. Exciton dissociation probabilities (P_{diss}) are calculated by the ratio of photocurrent density under short-circuit condition and saturated photocurrent density (J_{sc}/J_{sat}). Charge extraction efficiencies (P_{coll}) are evaluated by the ratio between photocurrent density under

the maximal power output condition and saturated photocurrent density (J_{ph}^{m}/J_{sat}), J_{ph} is defined as $J_{ph}=J_L-J_D$. J_L and J_D are the current densities under illumination and in the dark, respectively. V_{eff} is the effective voltage which is defined as V_0-V_{appl} in which V_0 is the voltage at $J_{ph}=0$ while V_{appl} represents the applied voltage bias. The different light intensities for light-intensity dependent J_{sc} and V_{oc} measurements are obtained using the different neutral filters, and the light intensity would be recalibrated using a standard Newport Oriel PN 91150 V Si diode when changing the neutral filter. Space-Charge-Limited-Current (SCLC) measurements were carried out using hole-only and electron-only diode configuration with the configuration of ITO/PEDOT:PSS/Active layer/MoO_3/Ag and ITO/ZnO/Active layer/PNDIT-F3N/Ag. PEDOT:PSS, PNDIT-F3N, and Ag layers were fabricated using the same procedure as the OSCs. MoO_3 was deposited to 10 nm by thermal evaporation in vacuum. ZnO was prepared through spin-coating its precursor onto the ITO glass substrate at 3500 rpm for 40 s, followed by a thermal annealing in air at 200 ℃ for 15 min. Subsequently, the carrier mobility in active layers were determined by fitting the dark current hole/electron-only devices to the SCLC model. The mobility was determined by the following equation: $J = 9\varepsilon_0\varepsilon_r\mu_0V^2/8L^3$. Where the J is dark current density, ε_r is the dielectric permittivity of the active layer (generally assumed to be 3 for organic materials), ε_0 is the dielectric permittivity of free space (ε_0= 8.854 ×10^{-12} F/m), L is the film thickness of active layers, μ_0 is the measured hole or electron mobility, and V is the voltage, which is defined as $V = V_{appl} - V_{bi}$, where V_{appl} is the applied voltage, V_{bi} is the built-in voltage. A digital source meter (Keithley 2400) and a picoammeter (Keithley 6482) were utilized for the electroluminescence external quantum efficiency (EQE_{EL}) measurements. The former was applied to inject electric current into the solar cells to emit the photons, which will be collected using a Si diode and form electric current that can be measured by the latter. For the electroluminescence (EL) measurement, a source meter was employed to create the injected electric current leading to the luminescence of the solar cells. After going through an optical fiber (BFL200LS02, Thorlab), the emitted light emerged from the solar cells was collected by a fluorescence spectrometer (KYMERA-3281-B2, Andor Technology) including two

sets of diffraction gratings for the wavelength range of 600-1100 nm and 900-1400 nm, and was measured by a Si EMCCD camera (DU970PBVF, Andor Technology) and an InGaAs camera (DU491A-1.7, Andor Technology), respectively. The EL spectra were corrected for the optical losses in the fibers, the spectrometer and the cameras, using a calibrated halogen lamp (HL-3P-CAL, Ocean Optics Germany GmbH).

Table S1. Optical and electrochemical data of PM6, PF8 and PF8-FSVA.

Polymer	Solution		Film			Cyclic Voltammetry		
	λ_{max} (nm)	ε (10^5 cm^{-1})	λ_{max} (nm)	λ_{onset} (nm)	E_g^{Opt} (eV)	E_{Ox} (V)	HOMO (eV)	LUMO[(a)] (eV)
PM6	575, 615	1.28	579, 620	675	1.837	0.75	-5.52	-3.68
PF8	576, 616	1.37	581, 623	676	1.834	0.78	-5.55	-3.72
PF8-FSVA	/	/	582, 625	677	1.832	/	/	/

[(a)] The LUMO energy levels of polymers are calculated as follows: $E_{LUMO} = E_{HOMO} + E_g^{Opt}$

Table S2. Molecular packing information of PM6, PF8 and PF8-FSVA films in out-of-plane direction from GIWAXS measurements.

Polymers	q (Å^{-1})	d-spacing (Å)	FWHM (Å^{-1})	CCL[(a)] (Å)
PM6	1.73	3.63	0.256	22.09
PF8	1.75	3.59	0.248	22.80
PF8-FSVA	1.76	3.57	0.242	23.37

[(a)] Crystal coherence length (CCL) was calculated according to Scherrer equation CCL = 2πK/Δq, where K is the shape factor (K=0.9) and Δq is the full width at half-maximum (FWHM) of diffraction peak.

Table S3. Photovoltaic parameters of PM6:L8BO based OSCs with different thicknesses and treated with FSVA at 100 ℃ for 3 min.

Thicknesses (nm)	V_{oc} (V)	J_{sc} (mA cm^{-2})	FF (%)	PCE (%)
110±10	0.894	25.68	78.46	18.01 (17.57±0.39)
300±10	0.878	25.93	71.45	16.26 (15.80±0.43)
500±10	0.862	25.04	64.71	13.97 (13.46±0.47)

Table S4. Photovoltaic parameters of 300-nm thick-film OSCs with different acceptors.

Active Layer	V_{oc} (V)	J_{sc} (mA cm^{-2})	*FF* (%)	PCE (%)
PM6:BTP-eC9	0.838	27.82	69.45	16.19 (15.72±0.48)
PF8:BTP-eC9	0.840	28.21	71.79	17.01 (16.54±0.43)
PF8:BTP-eC9 (FSVA)	0.842	28.34	72.61	17.33 (16.89±0.42)
PM6:Y6	0.830	27.25	67.79	15.33 (14.95±0.40)
PF8:Y6	0.834	27.71	70.11	16.20 (15.81±0.37)
PF8:Y6 (FSVA)	0.836	27.84	71.48	16.64 (16.30±0.36)

Table S5. Molecular packing information of 300-nm PM6:L8BO, PF8:L8BO and PF8:L8BO (FSVA) blend films in out-of-plane direction from GIWAXS measurements.

Active Layer	*q* (Å^{-1})	*d*-spacing (Å)	FWHM (Å^{-1})	CCL (Å)
PM6:L8BO	1.75	3.59	0.252	22.44
PF8:L8BO	1.77	3.55	0.245	23.08
PF8:L8BO (FSVA)	1.77	3.55	0.238	23.76

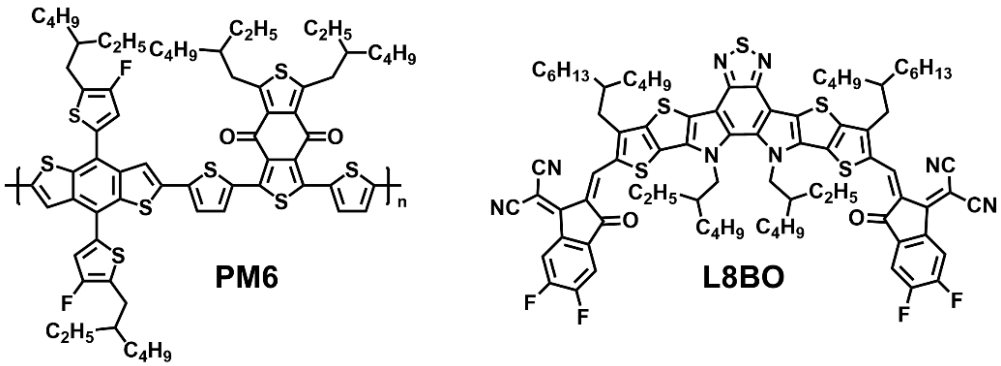

Fig. S1. Chemical structures of PM6 and L8BO.

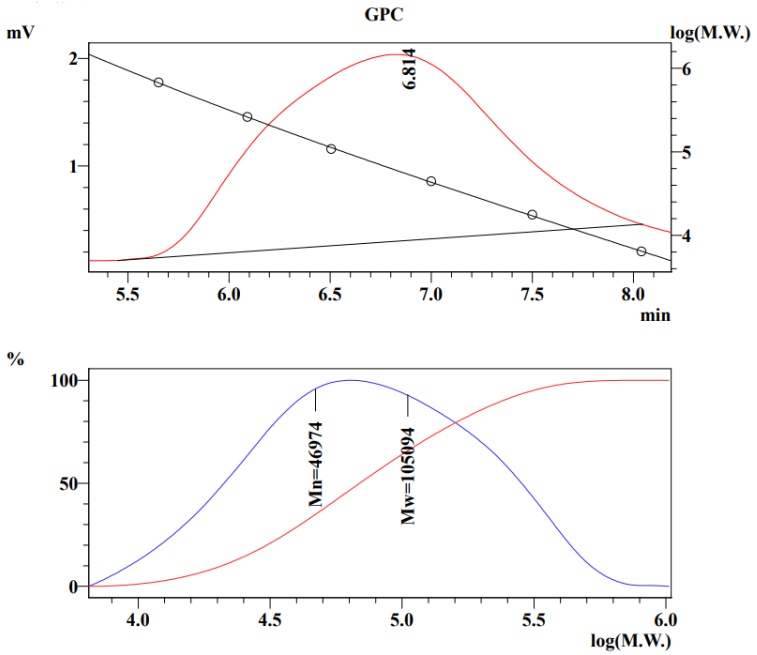

Fig. S2. Molecular weight and polydispersity index of PF8 calculated by GPC.

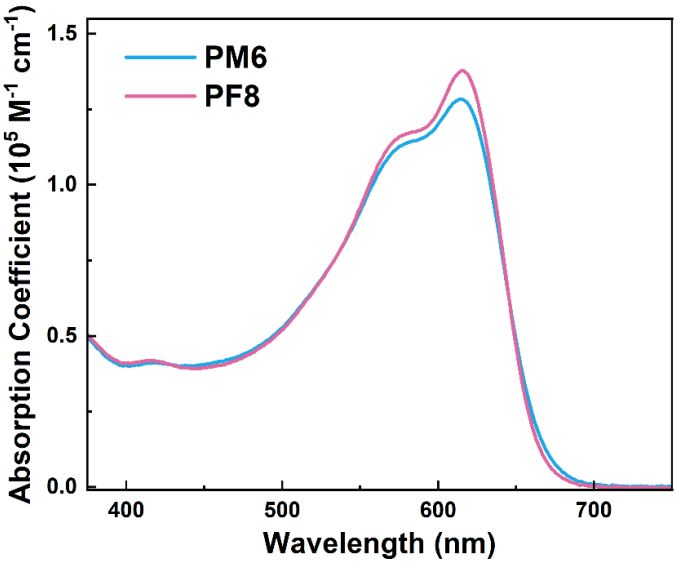

Fig. S3. Absorption spectra of PM6 and PF8 in chloroform solution.

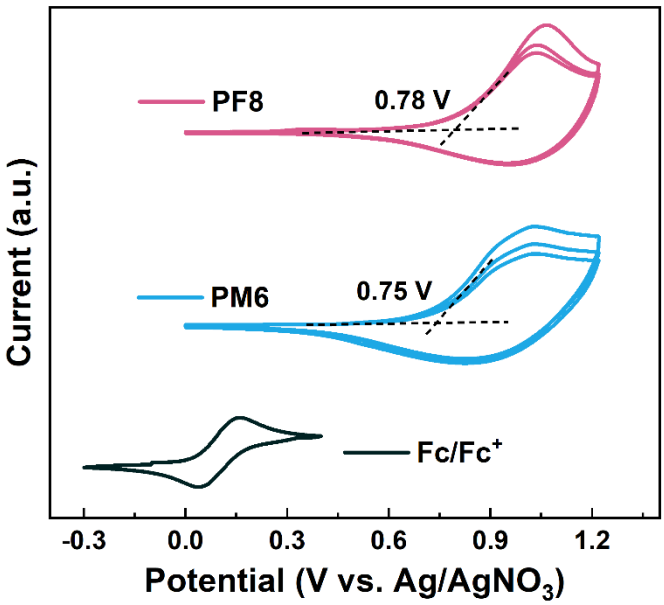

Fig. S4. Cyclic voltammograms of the PM6 and PF8 films with Fc/Fc^+ as the reference.

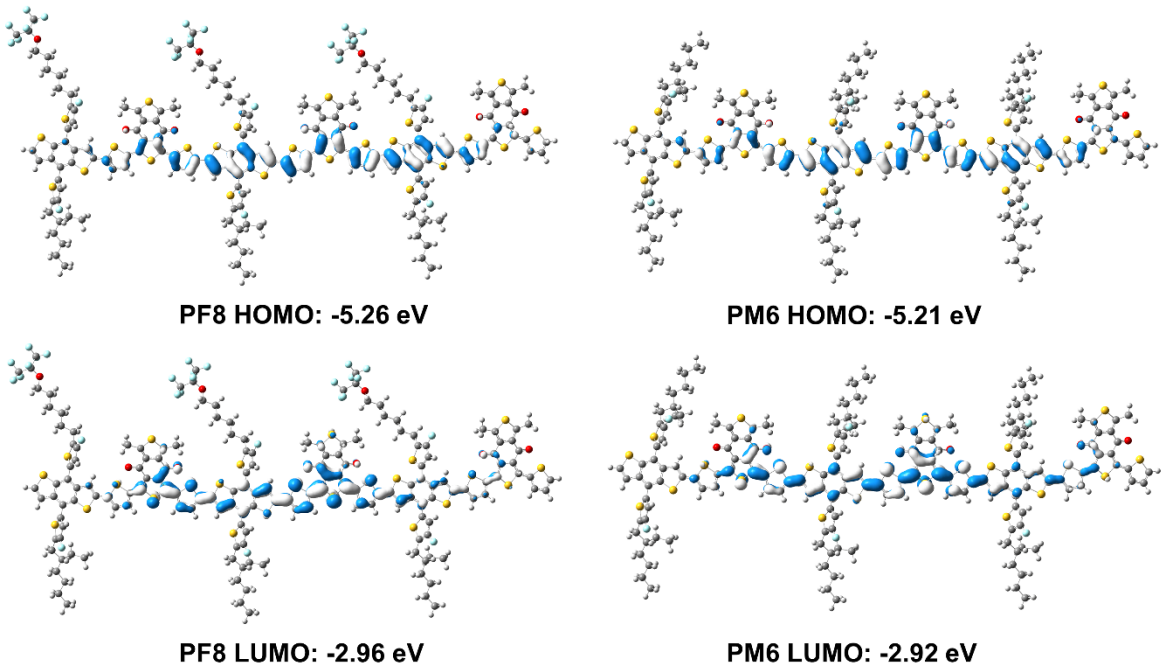

Fig. S5. Calculated HOMO/LUMO orbital energy levels of PF8 and PM6.

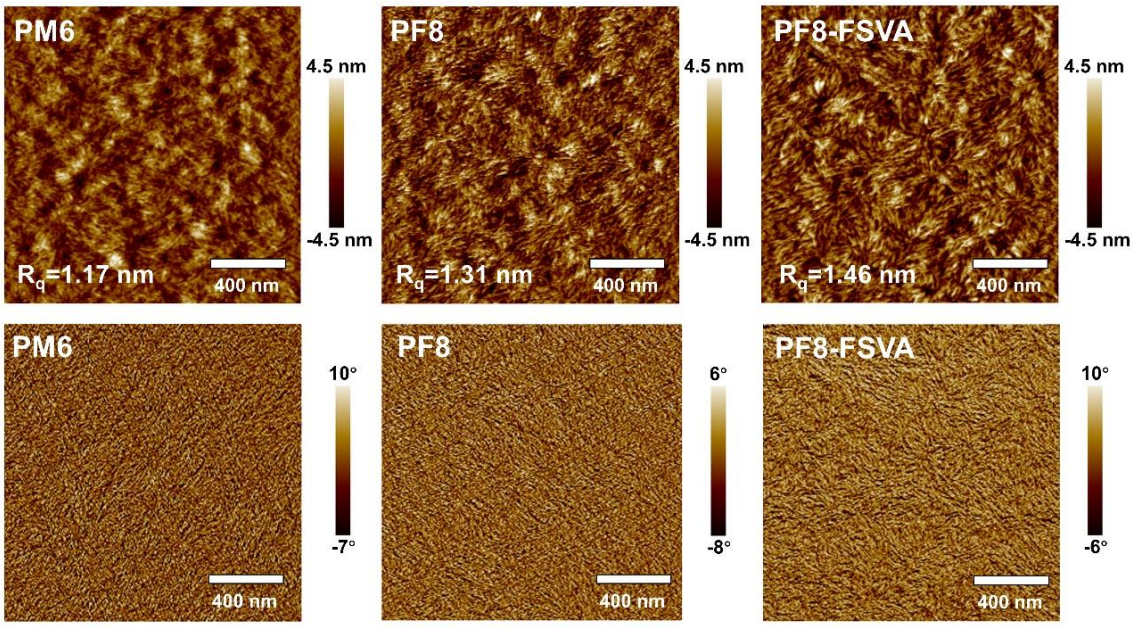

Fig. S6. AFM height and phase images of PM6, PF8 and PF8-FSVA films.

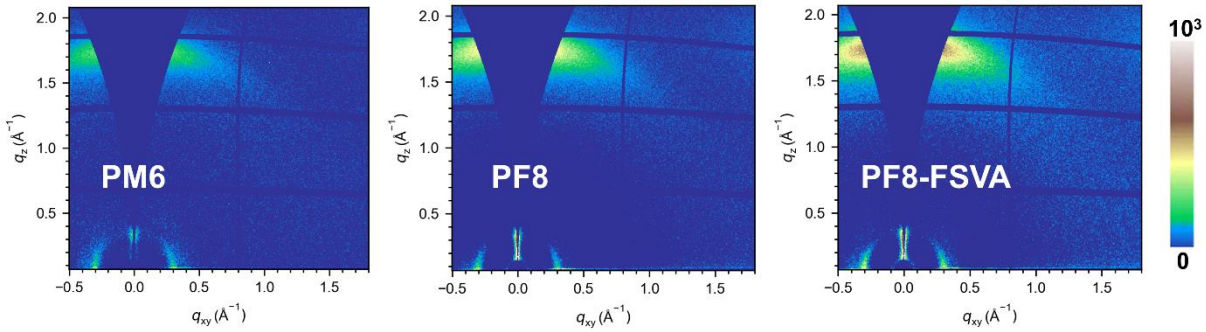

Fig. S7. 2D GIWAXS images of PM6, PF8 and PF8-FSVA films.

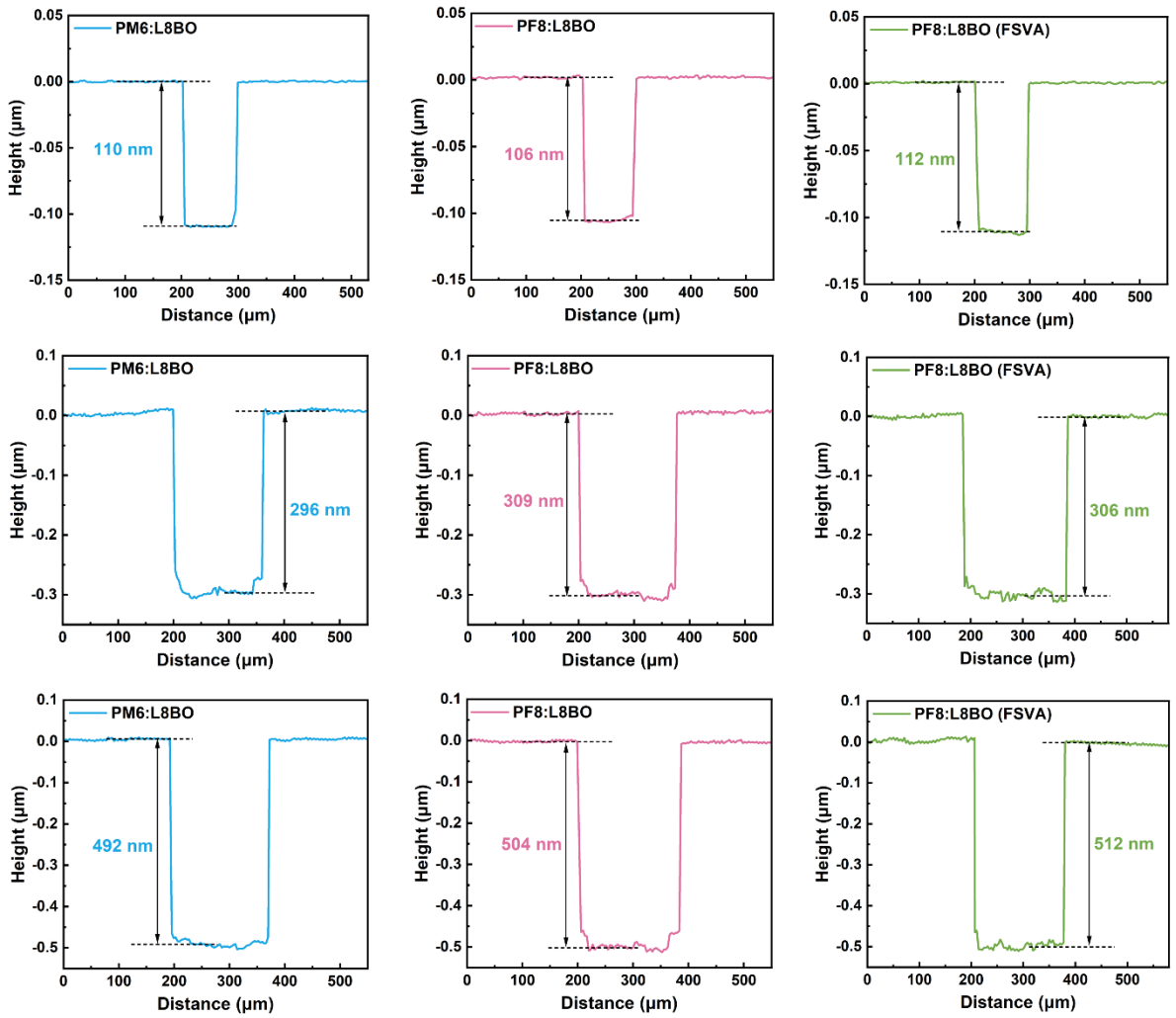

Fig. S8. Thicknesses of PM6:L8BO, PF8:L8BO and PF8:L8BO (FSVA) blend films.

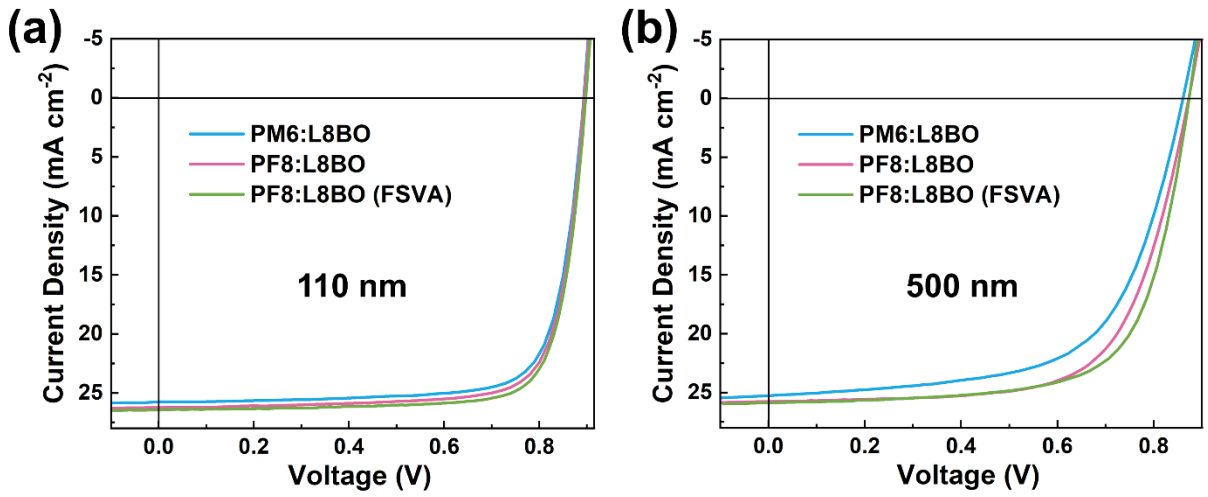

Fig. S9. *J-V* curves of thick-film OSCs with the thicknesses of (a) 110 nm and (b) 500 nm.

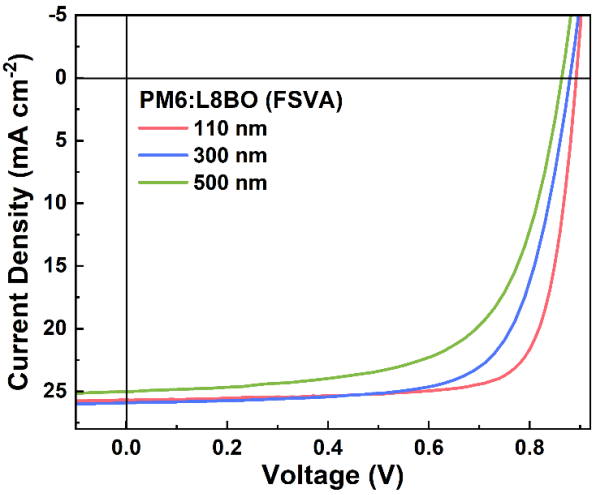

Fig. S10. *J-V* curves of FSVA-treated PM6:L8BO devices with different thicknesses.

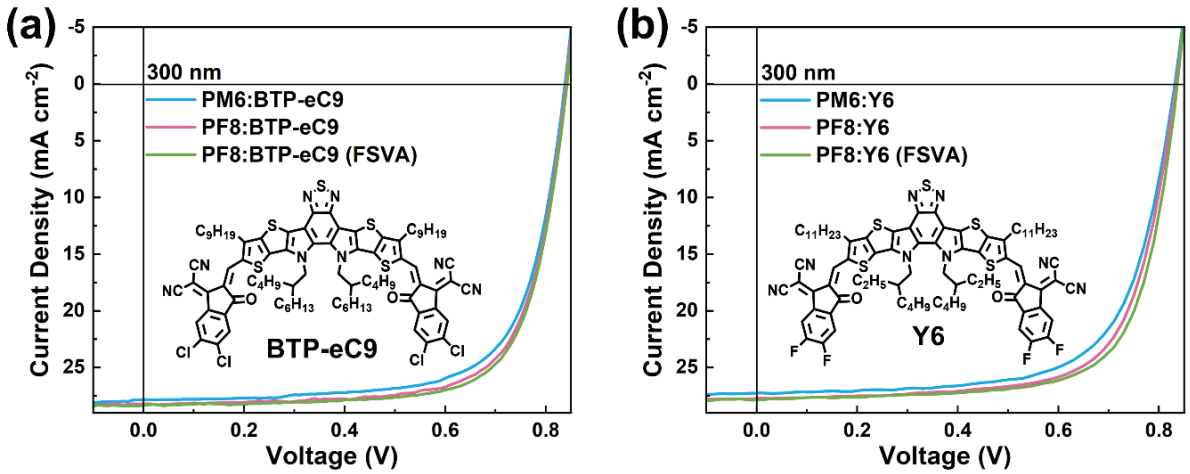

Fig. S11. *J-V* curves of 300-nm thick-film OSCs with different acceptors: (a) BTP-eC9 and (b) Y6.

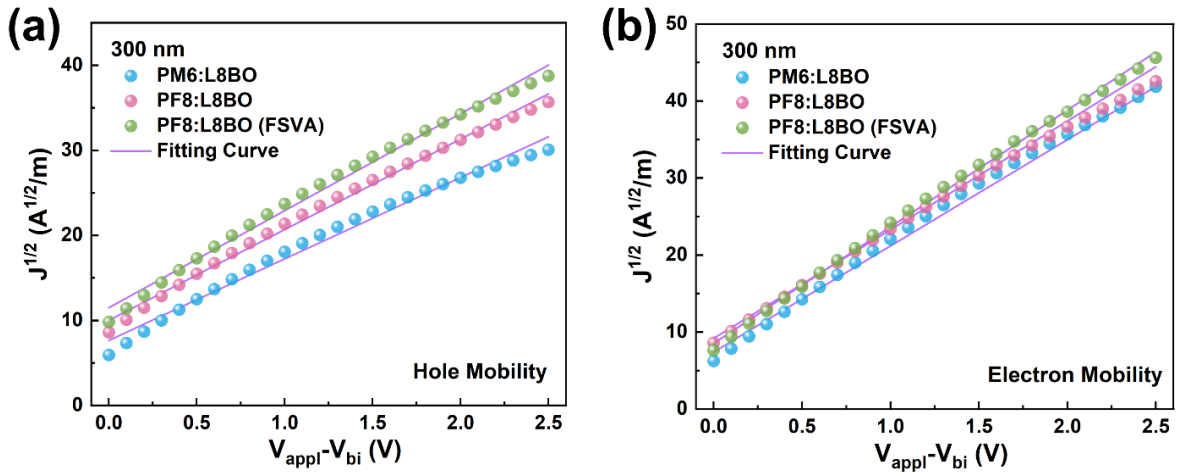

Fig. S12. Fitting *J-V* curves of (a) hole-only and (b) electron-only devices based on 300-nm PM6:L8BO, PF8:L8BO and PF8:L8BO (FSVA) active layer by SCLC models.

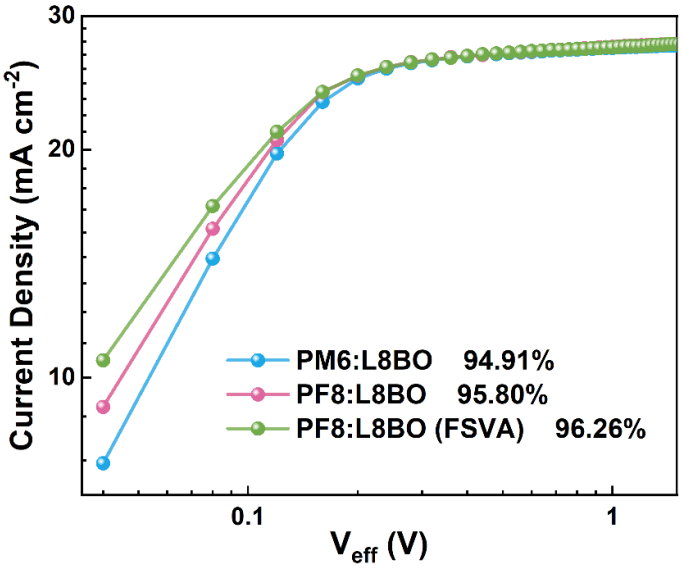

Fig. S13. The photocurrent density versus V_{eff} of the 300-nm PM6:L8BO, PF8:L8BO and PF8:L8BO (FSVA) devices.

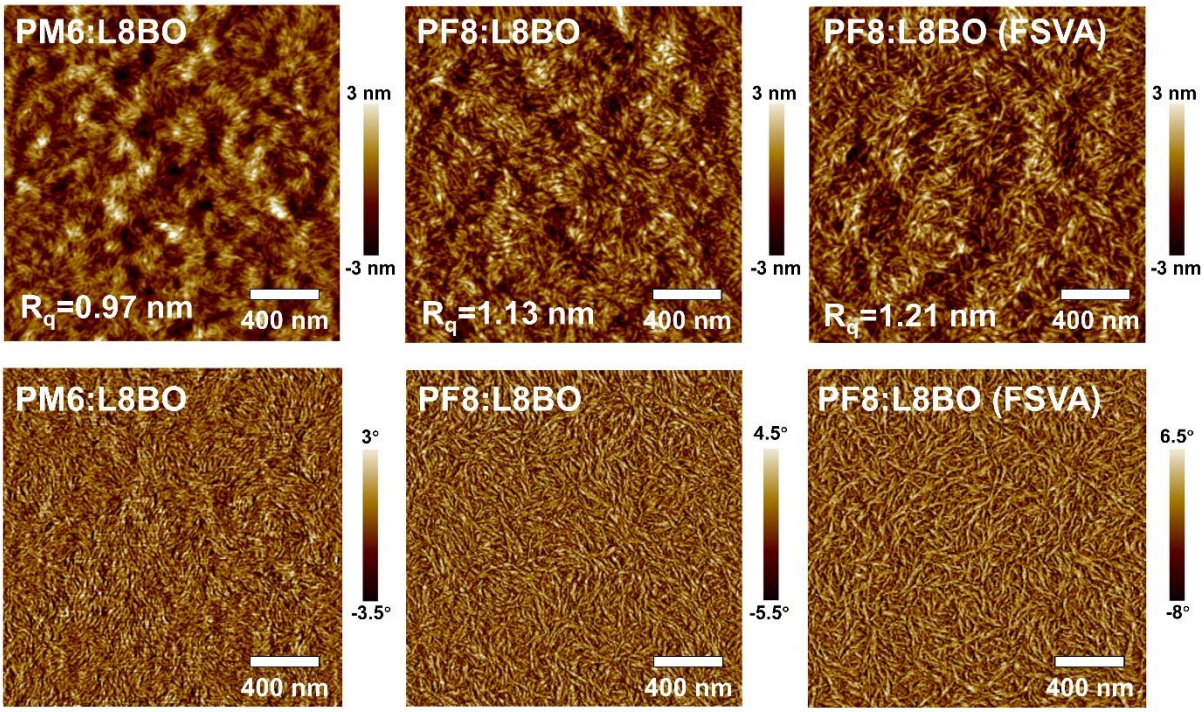

Fig. S14. AFM height and phase images of 300-nm PM6:L8BO, PF8:L8BO and PF8:L8BO (FSVA) based blend films.

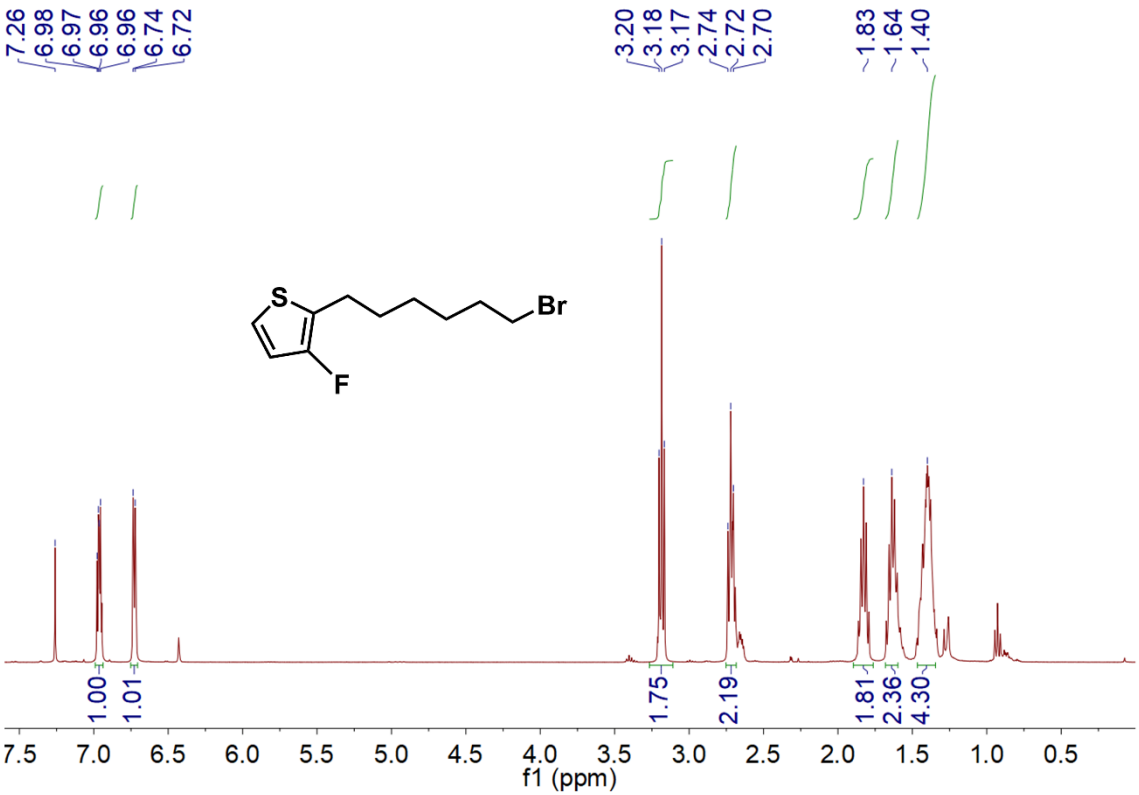

Fig. S15. ^{1}H NMR of Compound 2 in $CDCl_3$.

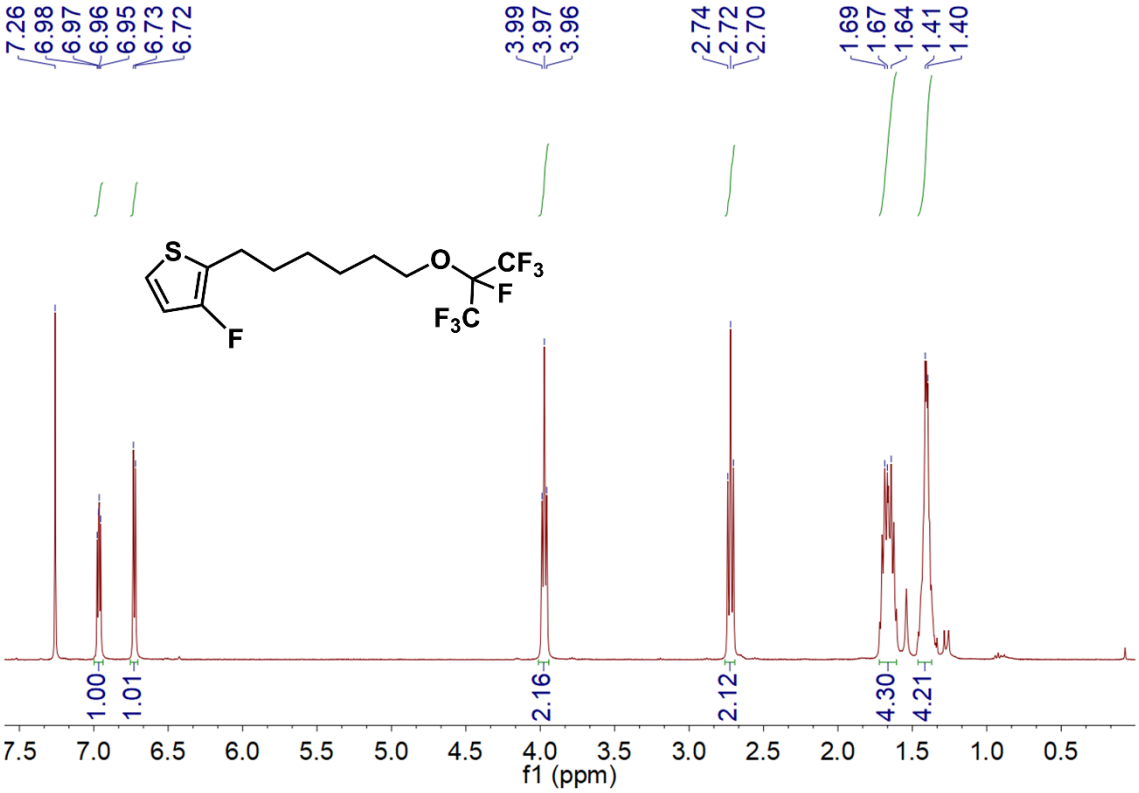

Fig. S16. ^{1}H NMR of Compound 4 in $CDCl_3$.

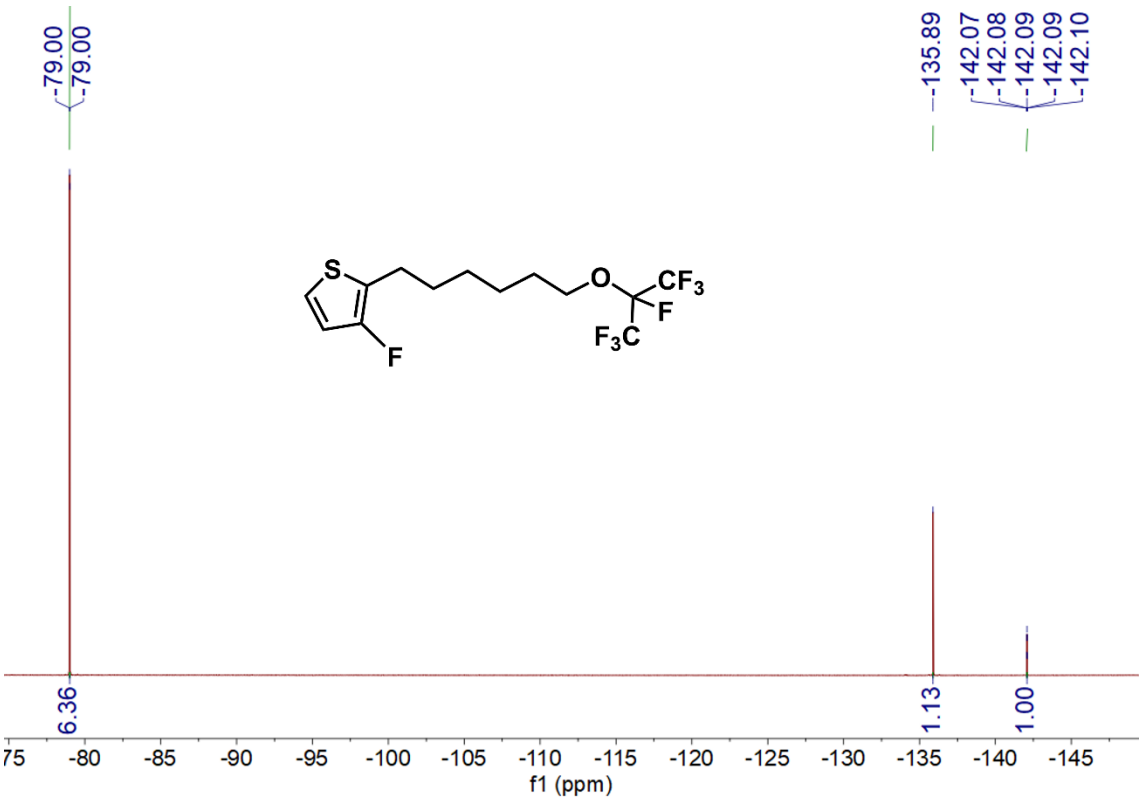

Fig. S17. ^{19}F NMR of Compound 4 in $CDCl_3$.

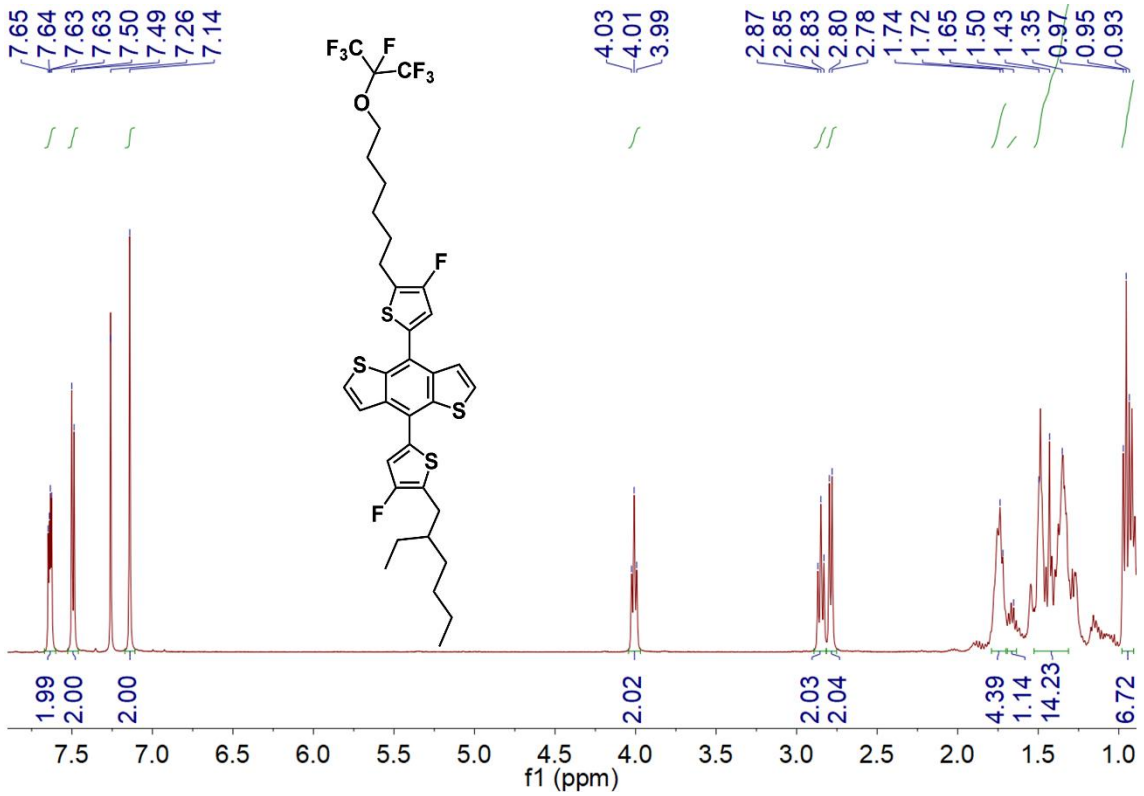

Fig. S18. ^{1}H NMR of Compound 5 in $CDCl_3$.

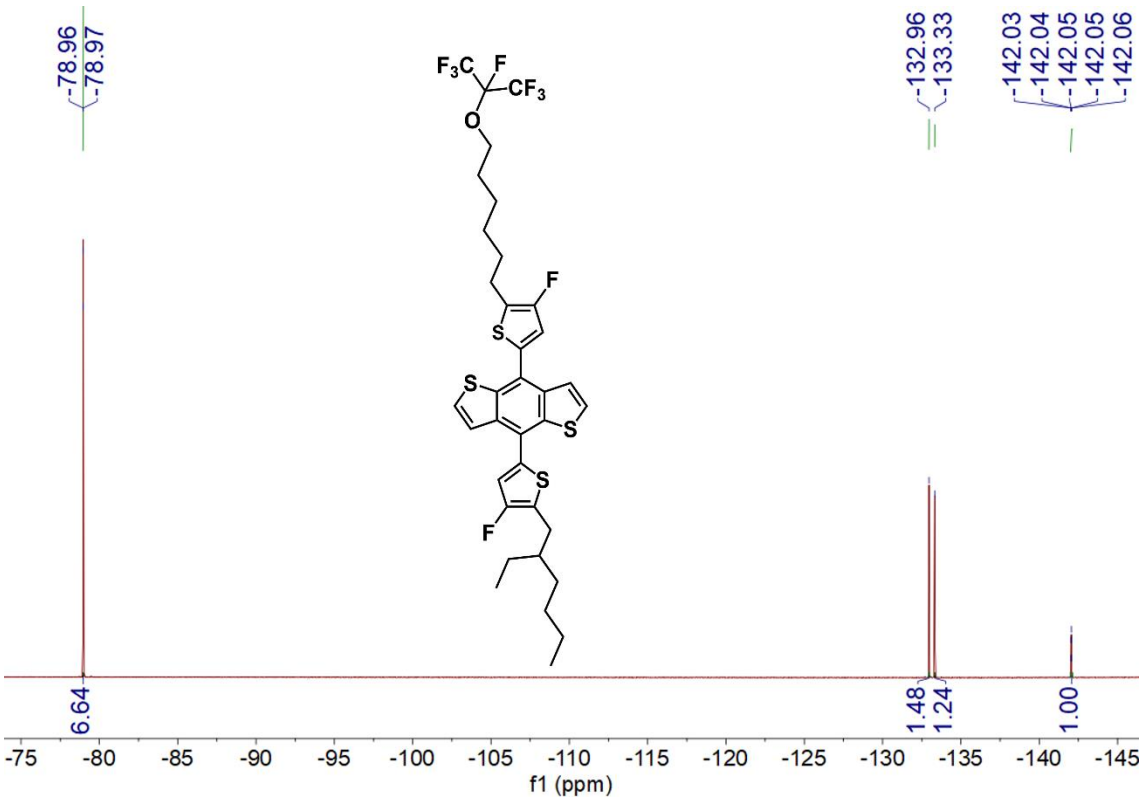

Fig. S19. ^{19}F NMR of Compound 5 in $CDCl_3$.

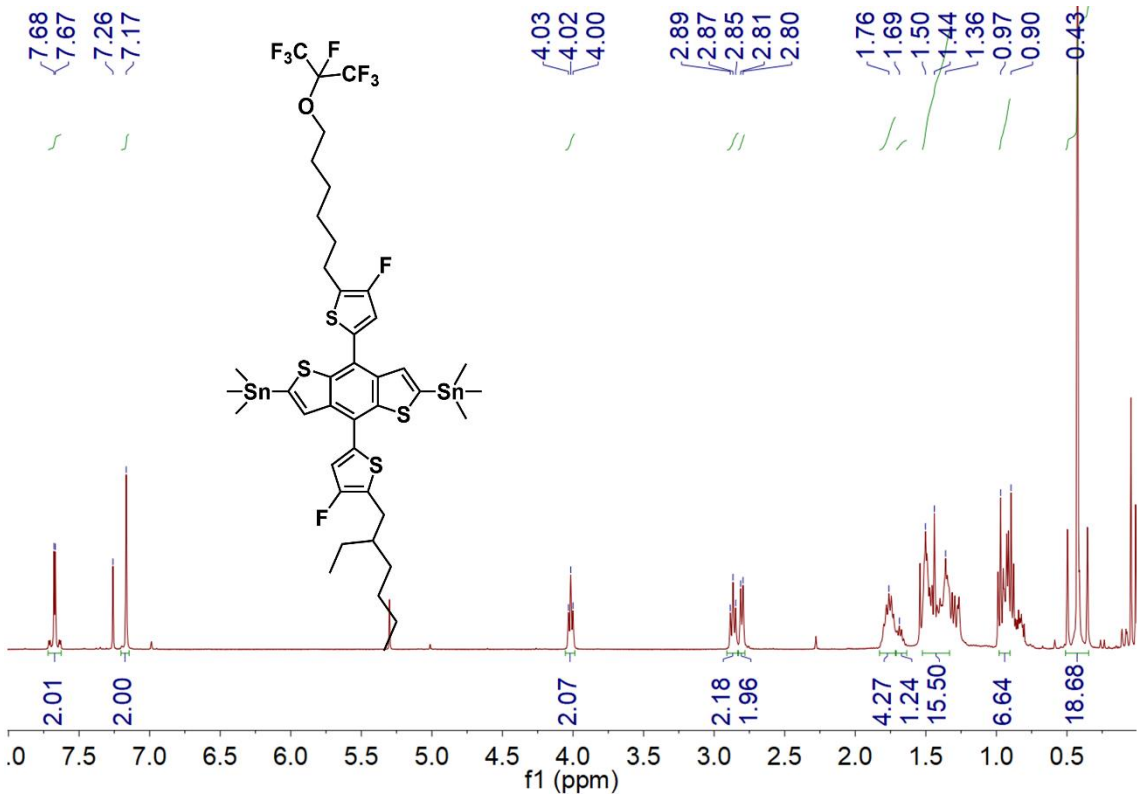

Fig. S20. ^{1}H NMR of FBDT-OF7 in $CDCl_3$.

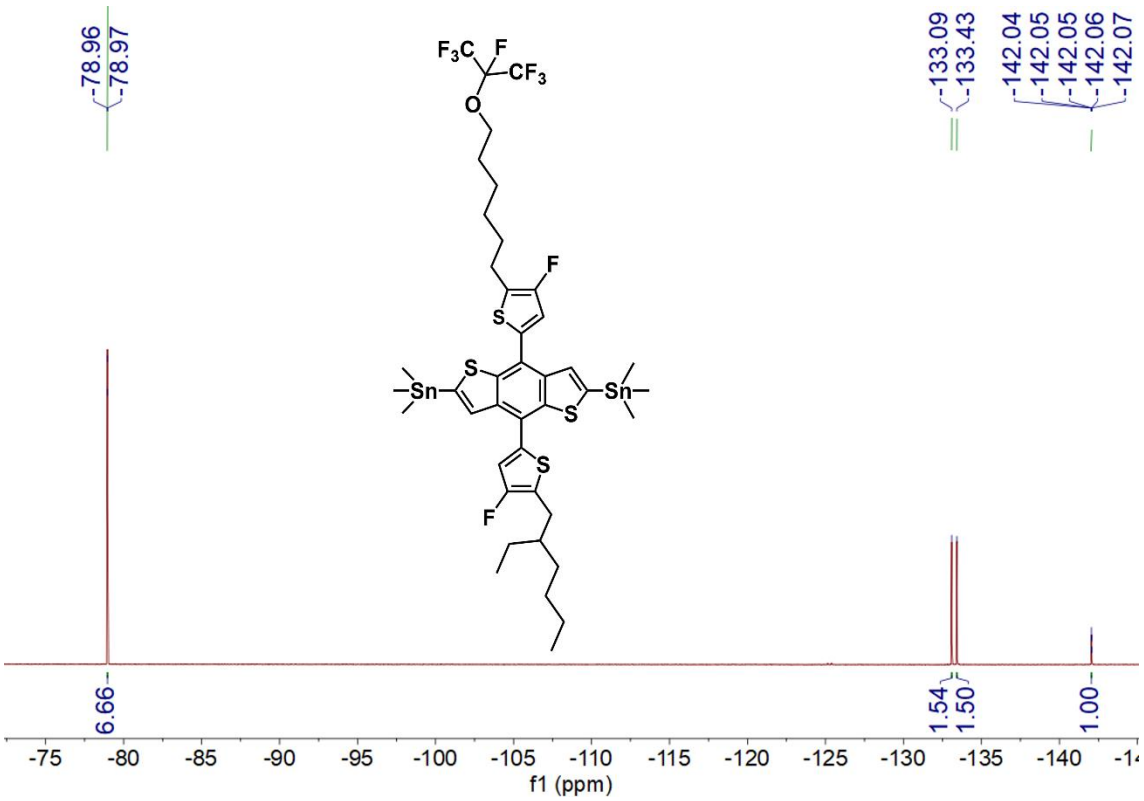

Fig. S21. ^{19}F NMR of FBDT-OF7 in $CDCl_3$.

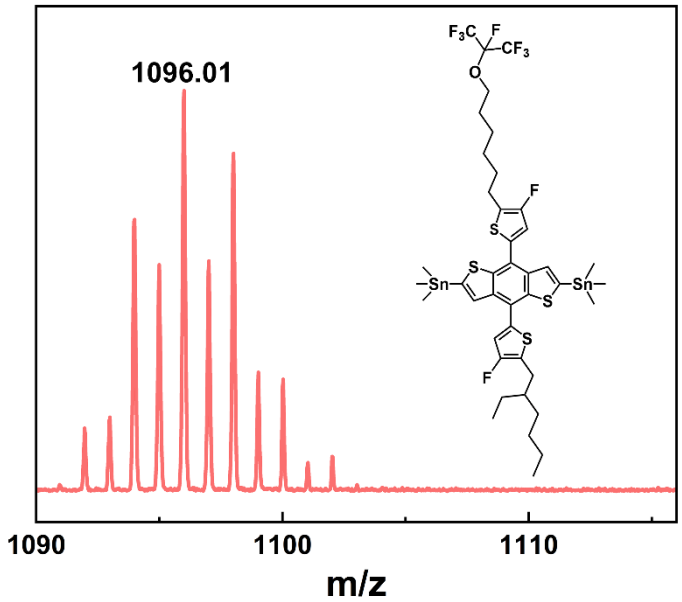

Fig. S22. MALDI-TOF MS analyses of FBDT-OF7.